Complement contributes to antibody-mediated protection against repeated SHIV challenge

Benjamin Goldberg, David Spencer, Shilpi Pandey, Tracy Ordonez, Philip Barnette, Yun Yu, Lina Gao, Jérémy Dufloo, Timothée Bruel, Olivier Schwartz, et al.

▶ **To cite this version:**

Benjamin Goldberg, David Spencer, Shilpi Pandey, Tracy Ordonez, Philip Barnette, et al.. Complement contributes to antibody-mediated protection against repeated SHIV challenge. Proceedings of the National Academy of Sciences of the United States of America, 2023, 120 (20), pp.e2221247120. 10.1073/pnas.2221247120 . pasteur-04165265

HAL Id: pasteur-04165265
https://pasteur.hal.science/pasteur-04165265

Submitted on 18 Jul 2023

HAL is a multi-disciplinary open access archive for the deposit and dissemination of scientific research documents, whether they are published or not. The documents may come from teaching and research institutions in France or abroad, or from public or private research centers.

L'archive ouverte pluridisciplinaire **HAL**, est destinée au dépôt et à la diffusion de documents scientifiques de niveau recherche, publiés ou non, émanant des établissements d'enseignement et de recherche français ou étrangers, des laboratoires publics ou privés.

Distributed under a Creative Commons Attribution - NonCommercial - NoDerivatives 4.0 International License

PNAS RESEARCH ARTICLE | IMMUNOLOGY AND INFLAMMATION

Complement contributes to antibody-mediated protection against repeated SHIV challenge

Benjamin S. Goldberg[a,1,2], David A. Spencer[b,1,3], Shilpi Pandey[b], Tracy Ordonez[b], Philip Barnette[b], Yun Yu[c,d], Lina Gao[c,d], Jérémy Dufloo[e,f,4], Timothée Bruel[e,g], Olivier Schwartz[e,g], Margaret E. Ackerman[a,h,5], and Ann J. Hessell[b,5]

Edited by Diane Griffin, Johns Hopkins University, Baltimore, MD; received December 14, 2022; accepted April 10, 2023

The first clinical efficacy trials of a broadly neutralizing antibody (bNAb) resulted in less benefit than expected and suggested that improvements are needed to prevent HIV infection. While considerable effort has focused on optimizing neutralization breadth and potency, it remains unclear whether augmenting the effector functions elicited by broadly neutralizing antibodies (bNAbs) may also improve their clinical potential. Among these effector functions, complement-mediated activities, which can culminate in the lysis of virions or infected cells, have been the least well studied. Here, functionally modified variants of the second-generation bNAb 10-1074 with ablated and enhanced complement activation profiles were used to examine the role of complement-associated effector functions. When administered prophylactically against simian-HIV challenge in rhesus macaques, more bNAb was required to prevent plasma viremia when complement activity was eliminated. Conversely, less bNAb was required to protect animals from plasma viremia when complement activity was enhanced. These results suggest that complement-mediated effector functions contribute to in vivo antiviral activity, and that their engineering may contribute to the further improvements in the efficacy of antibody-mediated prevention strategies.

HIV | neutralizing antibody | complement-dependent cytotoxicity | effector function | antibody engineering

A number of anti-HIV-1 broadly neutralizing antibodies (bNAbs) targeting highly conserved and vulnerable epitope regions of the envelope glycoprotein (Env) are being investigated in a range of clinical applications (1–3). Successful antibody prophylaxis aims to bypass frustrated vaccine development efforts, and the relatively long half-lives and tolerability profiles of bNAbs promise to offer an alternative to the disadvantages of the small-molecule inhibitors comprising current preexposure prophylaxis (PrEP) options (4–6).

To this end, repeated infusions of VRC01, a second-generation CD4-binding site-specific bNAb, were tested in large-scale human field trials designed to evaluate the efficacy of antibody-mediated prevention (AMP) of HIV-1 infection [HVTN 704/HPTN 085 (NCT02716675) and HVTN 703/HPTN 081 (NCT02568215)] (7). Mixed results were observed: Namely, while the VRC01-treated cohort was statistically at the same risk of infection as the placebo group overall, the rate of infection per 100 person-years was fourfold reduced in VRC01-treated subjects infected with viruses that were determined to be neutralization sensitive (IC80 <1 μg/mL), yielding an estimated level of protective efficacy of 75.4% (95% CI, 45.5 to 88.9). Given the suboptimal outcome of the AMP efficacy trial(s), improvements and novel approaches are needed. Beyond mining for novel antibody clones (8–11), efforts to optimize bNAb clinical performance have focused on improving plasma half-life and mucosal localization (12–18), neutralization potency and breadth (16, 19–25), and Fc-mediated effector function (26). Among these strategies, the value of the latter has been suggested from experiments in humanized mice (27–29), but is the least well established in the nonhuman primate (NHP) model.

In the context of HIV, antibody-mediated effector functions, including antibody-dependent cellular cytotoxicity (ADCC) and phagocytosis (ADCP), and complement activation—among others—have been reported to contribute to protective efficacy in mouse and NHP studies utilizing antibody Fc domain variants with ablated binding to Fc receptors (FcRs) and complement (27, 29–34). In the first study of its kind, Hessell et al. found that a loss-of-function variant of a first-generation bNAb reduced protection by 33% in (simian-HIV) SHIV-challenged NHP (30). In this and similar loss-of-function studies, observations that Fc functions contribute to protection have been observed across a range of bNAbs (30, 33, 35, 36), are more pronounced at subneutralizing bNAb titers (31), and appear to not contribute to the protection afforded by all bNAbs (37, 38).

Significance

Many tools exist to improve antibody effector function in vitro. While these protein engineering approaches have improved efficacy in mouse models, proof of improved activity in primates has been lacking. Here, in the rhesus macaque model, we report improvement to the in vivo antiviral activity of 10-1074, a clinically relevant HIV-neutralizing antibody, that results from Fc engineering to enhance complement cascade induction. We observe that lower levels of antibody and neutralization activity are observed at the time of plasma viremia for an antibody variant with improved complement activity, providing evidence that this mechanism may contribute to restricting spreading infection. These results support clinical investigation of Fc engineering for the many disease states in which antibody effector function contributes to mechanism.

The authors declare no competing interest.

This article is a PNAS Direct Submission.

Copyright © 2023 the Author(s). Published by PNAS. This article is distributed under Creative Commons Attribution-NonCommercial-NoDerivatives License 4.0 (CC BY-NC-ND).

[1]B.S.G. and D.A.S. contributed equally to this work.

[2]Present address: Flagship Labs 72 Inc., Cambridge, MA 02139.

[3]Present address: Absci Corp, Vancouver, WA 98683.

[4]Present address: Institute for Integrative Systems Biology (I2SysBio), Universitat de València-CSIC, 46980 València, Spain.

[5]To whom correspondence may be addressed. Email: margaret.e.ackerman@dartmouth.edu or hessell@ohsu.edu.

This article contains supporting information online at https://www.pnas.org/lookup/suppl/doi:10.1073/pnas.2221247120/-/DCSupplemental.

Published May 8, 2023.

Downloaded from https://www.pnas.org by INSTITUT PASTEUR MEDIATHEQUE SCIENTIFIC on July 19, 2023 from IP address 157.99.174.25.

Relevant to the need to improve bNAb activity, whether the augmentation of HIV bNAb-mediated effector functions through Fc engineering can improve bNAb protective efficacy in vivo remains an open question. Protection studies in a humanized mouse model have demonstrated that while it is possible to leverage Fc modifications to improve protection outcomes against HIV (27, 29), similar studies in NHPs have not demonstrated such benefit (26, 32).

Among effector functions, complement-associated antiviral activities are the least well studied. This lack of emphasis may result from the seminal study of mechanism(s) of action of the prototype bNAb, b12, in which modification to abolish complement activation potential ("KA;" K322A) demonstrated no loss of protection in an NHP model (30). However, follow-up studies have since demonstrated that unmodified b12 possesses the same complement-null phenotype as the KA variant in assays against virions and Env-expressing cells (39, 40), suggesting the potential value of further evaluations in animal models. Whereas most passive transfer studies have evaluated mAbs with compromised binding to both FcγR and the complement cascade initiator C1q (29, 30, 35, 37, 38), a recent protection study revealed a significant increase in infected CD4+ T cells in humanized mice passively immunized with a complement-null variant of the weakly neutralizing V3-directed mAb, 2219, compared to the unmodified 2219 (34). An attempt to improve antiviral complement contributions in another weakly neutralizing setting with MPER-directed bNAb 10E8v4 gave inconclusive results, as 10E8v4 with enhanced binding to C1q and FcγR was rapidly cleared from plasma (33). Collectively, further studies are needed to resolve the ability of Fc engineering in general, and complement-associated activities in particular, to improve in vivo outcomes.

Given these open questions, we sought to further investigate the contribution of antibody-mediated activation of complement to the protective potency of an HIV bNAb, 10-1074, in passive transfer and SHIV challenge experiments in the NHP model.

Results

10-1074 mAb Panel with Enhanced and Reduced Capacity to Activate Complement. We selected the V3 loop-directed bNAb, 10-1074 (41), to be a suitable candidate for investigating the role of complement, if any, in protection from SHIV infection in NHP passive immunization studies based on its high degree of complement activity relative to a panel of clinically relevant bNAbs (39) across a range of in vitro assessments (40). Using complement-specific enhancing and ablating modifications, we aimed to probe whether, in the context of relatively high Fc polyfunctionality, complement contributed to antiviral activity in vivo. Point mutations that have been previously reported to either directly abrogate ("KA," K322A) (42) or to indirectly enhance C1 complex recruitment and subsequent complement activation via favoring Fc domain hexamerization ("EG," E430G) (43), were made in the IgG1 backbone of 10-1074 by site-directed mutagenesis (Fig. 1*A*). Importantly, this strategy for improving complement-mediated antibody effector function has been previously validated in vivo (44, 45) and is currently under clinical investigation (NCT03576131, NCT04824794, NCT04358458). Additionally, while human and rhesus C1q are well conserved, we hypothesized that this modification would function independently of the affinity of rhesus C1q for human IgG1 given that improvement in function is driven by favoring IgG hexamerization rather than directly improving intrinsic affinity for each of the six globular heads of C1q. Relative to unmodified 10-1074, these mutations did not appreciably modify affinity for cognate antigen ($gp140_{YU2}$ trimer), soluble rhesus macaque FcγRs (IA, IIA-1, IIB-1, IIIA-1), or FcRn, as measured by biolayer interferometry (BLI) (Fig. 1*B*). Critically, neither Fc modification impacted the neutralization potency of 10-1074 against $SHIV_{SF162P3}$, the replication-competent challenge virus used in this study (Fig. 1*C* and *SI Appendix*, Fig. S1). Unmodified 10-1074 displayed high FcγR-dependent functionality, and corroborating the FcγR-binding profiles, the modifications did not alter ADCC or ADCP activities (Fig. 1 *D* and *E*).

In contrast, the C1q-binding knockout variant, KA, displayed near-baseline activity in most in vitro functional measures of complement activity (Fig. 1 *F* and *G*). Unmodified 10-1074 displayed a dose-dependent recruitment of C1q to bNAb-opsonized antigen-conjugated beads, and the EG variant showed improved C1q recruitment in the context of multiple antigenic strains, an effect that was most pronounced for trimeric gp140 (Fig. 1*F*). Unmodified 10-1074 mediated dose-dependent lysis of virions, and whereas the KA variant showed no activity, the target-dependent hexamer favoring EG variant showed potentiated virion lysis (Fig. 1*G*). Additionally, cells expressing varying levels of Env were more efficiently lysed by the EG variant, than by WT, which in turn exhibited greater activity than that of the KA variant (Fig. 1*H*).

10-1074 Variants Provide Protection from Repeated Low-Dose SHIV Challenge. Given improved resolution to detect the contribution of Fc-associated mechanisms of action expected when bNAbs are evaluated at subneutralizing titers (37, 38, 46), we selected a moderate mAb dose (4 mg/kg) delivered subcutaneously 3 d prior to initiating repeated weekly low-dose (30 $TCID_{50}$) $SHIV_{SF162P3}$ viral challenge (Fig. 2*A*). We hypothesized that incomplete neutralization might be supplanted by the combined contributions of strong FcγR-mediated and complement-mediated activities of 10-1074, resulting in the ability to improve infection resistance or viremic control.

Infection outcomes varied across the 10-1074-treated NHP groups, but all animals were infected by the end of the challenge series (Fig. 2*B*). Unmodified 10-1074 delayed infection with a 14% (1/7) infection rate by week 4 compared to 100% (6/6) of the isotype control-treated group. Three of six macaques treated with the control antibody experienced breakthrough infection after the initial challenge and all the six were infected following the third-weekly challenge. In contrast, treatment with 10-1074, 10-1074.KA, and 10-1074.EG resulted in the protection of at least one animal for up to 16-, 12-, and seven-weekly challenges, respectively. Analysis of longitudinal protection revealed that 10-1074 and 10-1074.KA each provided equivalent levels of protective durability, with each group displaying a median of 10-weekly challenges to breakthrough (Fig. 2*C*). In contrast, despite its improved function in vitro, the 10-1074.EG-treated group showed reduced resistance to challenge relative to either unmodified 10-1074 mAb ($P = 0.0099$) or 10-1074.KA ($P = 0.037$), displaying breakthrough following a median of six SHIV challenges.

Following infection, acute or postacute viremia can be useful measures indicative of the ability of treatment to impact viral establishment, which can influence the course of disease. No significant differences in either peak plasma viral load (PVL) (Fig. 2*D*) or set-point viremia (Fig. 2*E*) were observed between groups.

Effect of Fc Mutations on bNAb Pharmacokinetics (PK). At face value, these results suggest that complement-dependent effector function, as queried through Fc domain engineering, is irrelevant to or may contribute to increased infection risk. However, both

Downloaded from https://www.pnas.org by INSTITUT PASTEUR MEDIATHEQUE SCIENTIFIC on July 19, 2023 from IP address 157.99.174.25.

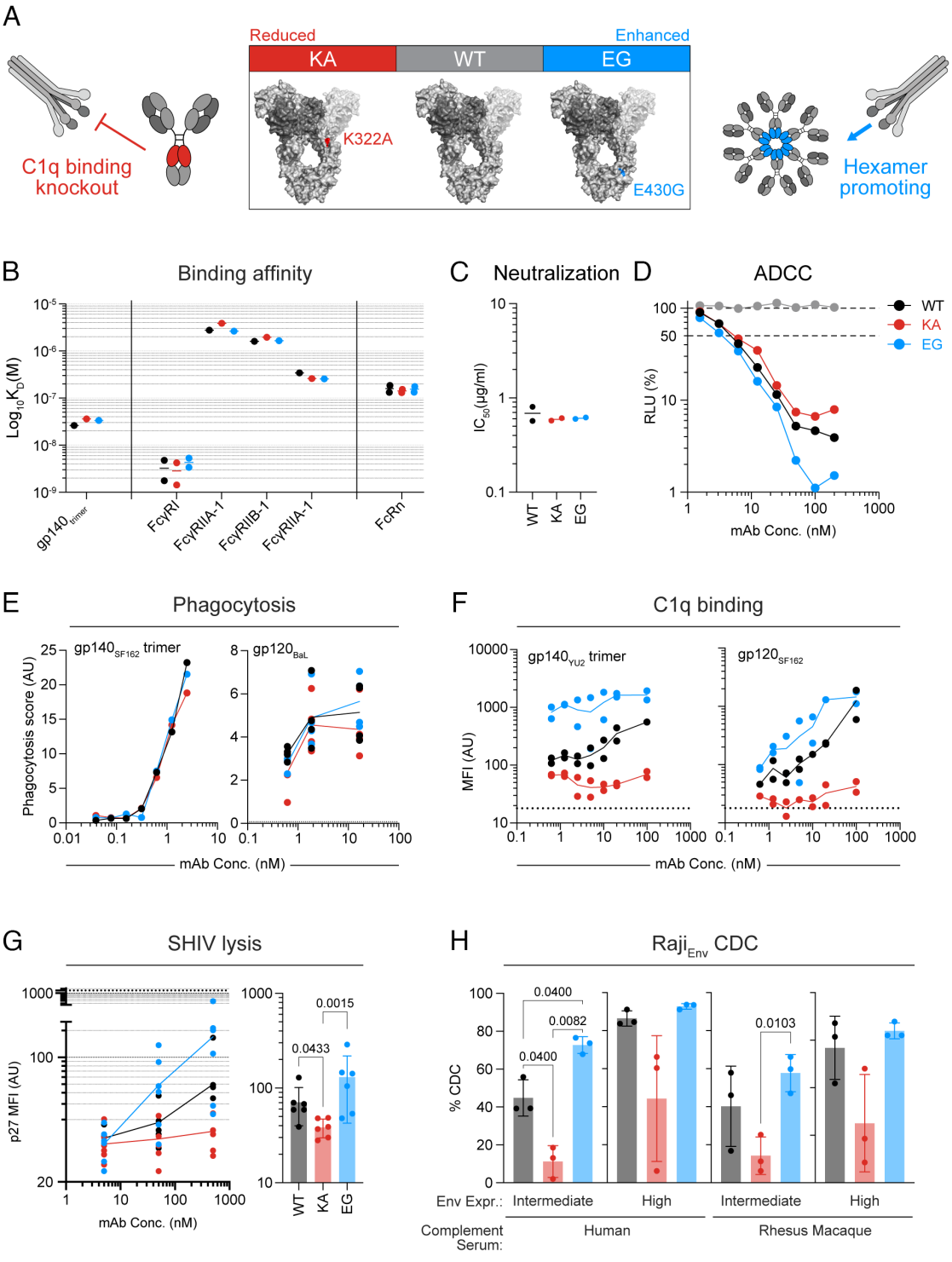

Fig. 1. Fc variants KA/EG specifically abrogate/enhance complement activity in bNAb 10-1074. (*A*) Overview of 10-1074 variants. Location and identity of Fc point mutations conferring reduced and enhanced complement activation. (*B*) Equilibrium dissociation constants characterizing the relative strength of biophysical interactions between the 10-1074 panel with a range of rhesus macaque Fc receptors and HIV-1 antigen. (*C*) Neutralization of replication- competent challenge virus, $SHIV_{SF162P3}$, by 10-1074 variant panel (single-round infection in TZM- bl cells) reported as 50% inhibitory concentration, IC50. Data shown represent experimental replicates conducted on different days by different operators. (*D*) ADCC activity against $SHIV_{SF162P3}$- infected target cells expressing a tat-inducible luciferase reporter. Activity reported as percent loss of relative light units (RLU). Anti-DEN3 (gray) displayed as negative control. (*E*) Phagocytic activity of 10-1074 as measured by rhesus PBMC internalization of antigen-conjugated fluorescent beads. Each dot represents PBMCs obtained from an individual monkey. (*F*) C1q recruited from rhesus macaque serum by the antibody-opsonized antigen beads, detected with an anti-human C1q antibody reagent. Two representative antigens are shown. Each point represents serum from an individual macaque (n = 2). (*G*) Antibody-dependent complement-mediated lysis of replication-competent $SHIV_{SF162P3}$ virions in complement-preserved rhesus serum derived from individual rhesus macaques (n = 6). Dotted line indicates 100% lysis. *Right* panel shows breakout for comparison at 500 nM condition. (*H*) Complement-mediated lysis of Raji cells expressing intermediate or high levels of HIV_{YU2} Env. Antibody-plus cells were incubated with human (*Left*) or rhesus macaque (*Right*) serum and the percentage of lysed cells was determined by flow cytometry. Results are reported as the percentage of dead cells above that in wells without antibody, with biological replicates from three independent serum donors. Statistical comparisons were performed using one-way ANOVA (corrected for multiple comparisons) using nonparametric Friedman test (*G*), and repeated-measures one-way ANOVAs with the Geisser–Greenhouse correction (*H*) and the Holm–Šidák correction for multiple comparisons. Statistical significance was determined using an alpha level of 0.05 and performed in GraphPad Prism 9.4.1. gC1q globular head domain of C1q, ADCC antibody-dependent cellular cytotoxicity, ADCML antibody-dependent complement-mediated lysis.

Downloaded from https://www.pnas.org by INSTITUT PASTEUR MEDIATHEQUE SCIENTIFIC on July 19, 2023 from IP address 157.99.174.25.

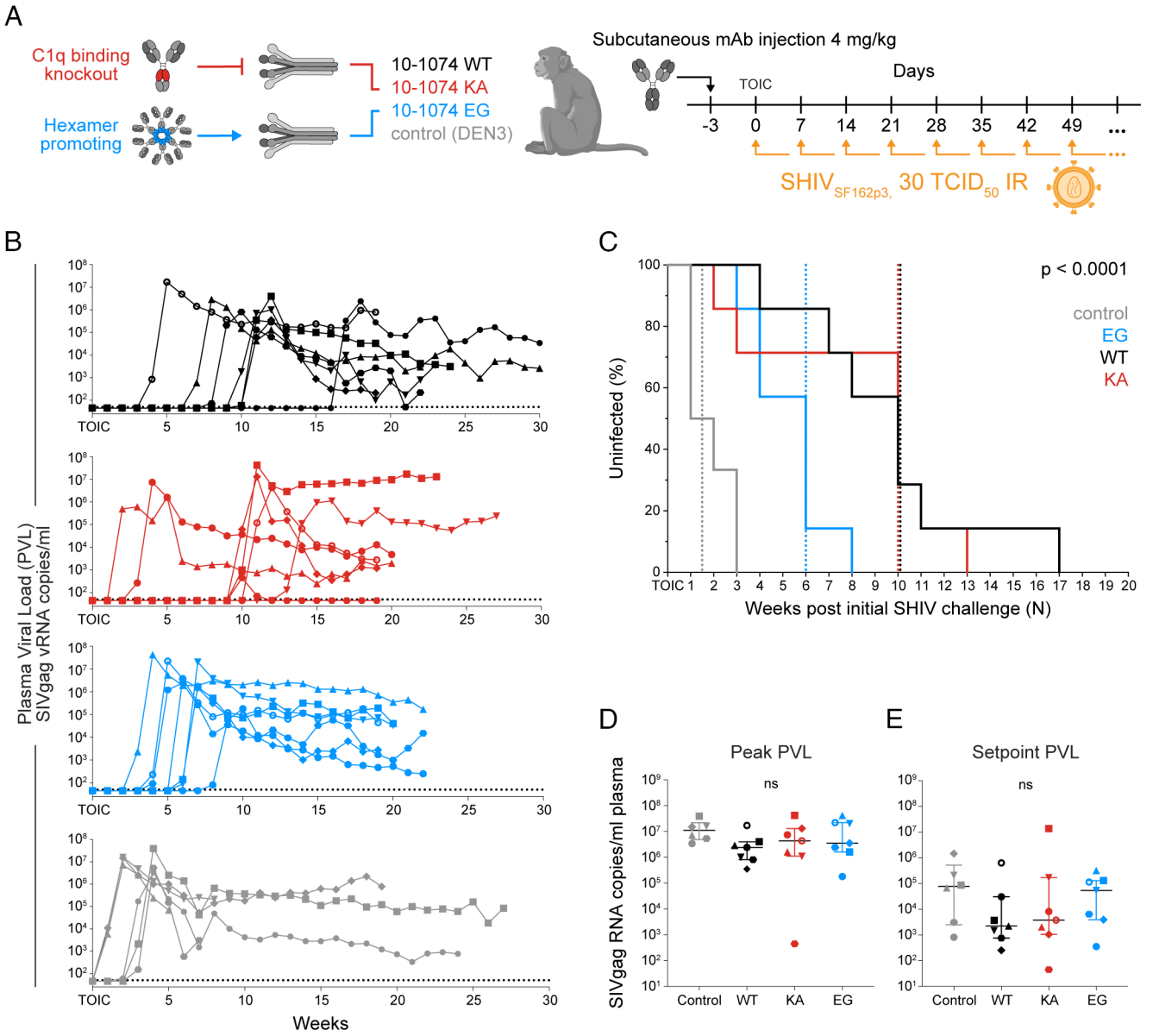

Fig. 2. Durability of protection is impacted by Fc mutations impacting complement activation. (*A*) Schematic of macaque challenge experiment (n = 6 for isotype control, n = 7 for each 10-1074 variant). (*B*) Individual plasma PVL over time separated by bNAb-treated group. (*C*) Survival analysis reporting percent breakthrough status of each group as a function of time. Median number of weekly challenges posttime of initial challenge (TOIC) to breakthrough displayed as vertical dotted line. (*D* and *E*) Median peak (*D*) and postacute (setpoint) (*E*) viremia. Statistical comparisons were performed using the log-rank (Mantel–Cox) test for survival analysis (*C*) and ordinary one-way ANOVA followed by Tukey's post-hoc correction for multiple comparisons (*D* and *E*), respectively. Statistical significance was determined using an alpha level of 0.05 and performed in GraphPad Prism 9.4.1. For experiments in which no statistically significant difference was determined from the respective tests, "ns" is displayed. PVL plasma viral load, $TCID_{50}$ 50% tissue culture infectious dose, IR intrarectal.

longitudinal PK profiles differed (Fig. 3 *A* and *B*) and serum bNAb levels detected as soon as 3 to 7 d post subcutaneous administration were lower for the EG variant as compared to either 10-1074 and 10-1074.KA (Fig. 3*C*). At the time of initial challenge, the median concentration of 10-1074.EG was threefold lower than that observed for unmodified 10-1074 and 10-1074.KA. This intergroup PK discrepancy not only persisted but also grew, resulting in approximately fivefold and sevenfold lower levels of EG present at weeks one and two, respectively, as compared to unmodified 10-1074 ($P = 0.0153$, $P < 0.0001$). In contrast, despite an animal with a strong and early antidrug antibody (ADA) response (*SI Appendix*, Fig. S2 *A–C*), 10-1074.KA was maintained at roughly twofold higher levels than unmodified 10-1074 at these early timepoints. Over the course of the challenge series, EG showed faster serum clearance relative to 10-1074 IgG1 (Fig. 3*D*).

As is frequently observed following even single infusions of human bNAbs in NHP, ADA responses were detected in seven animals (*SI Appendix*, Fig. S2 *A–C*). Of these, ADA responses were associated with undetectable levels of bNAb in four animals and dramatically reduced levels in an additional two animals prior to infection (*SI Appendix*, Fig. S2*B*). Rates of ADA responses were similar across treatment groups (2-3 animals per 10-1074 variant).

Reduced Neutralizing Titer but Enhanced Complement-Mediated Lysis of 10.1074.EG at the Time of Initial Challenge. To gain insight as to what impact the differences in antibody concentration at the onset of challenge had on antibody function, macaque serum collected prior to antibody administration was compared functionally with serum collected at the time of initial challenge.

Downloaded from https://www.pnas.org by INSTITUT PASTEUR MEDIATHEQUE SCIENTIFIC on July 19, 2023 from IP address 157.99.174.25.

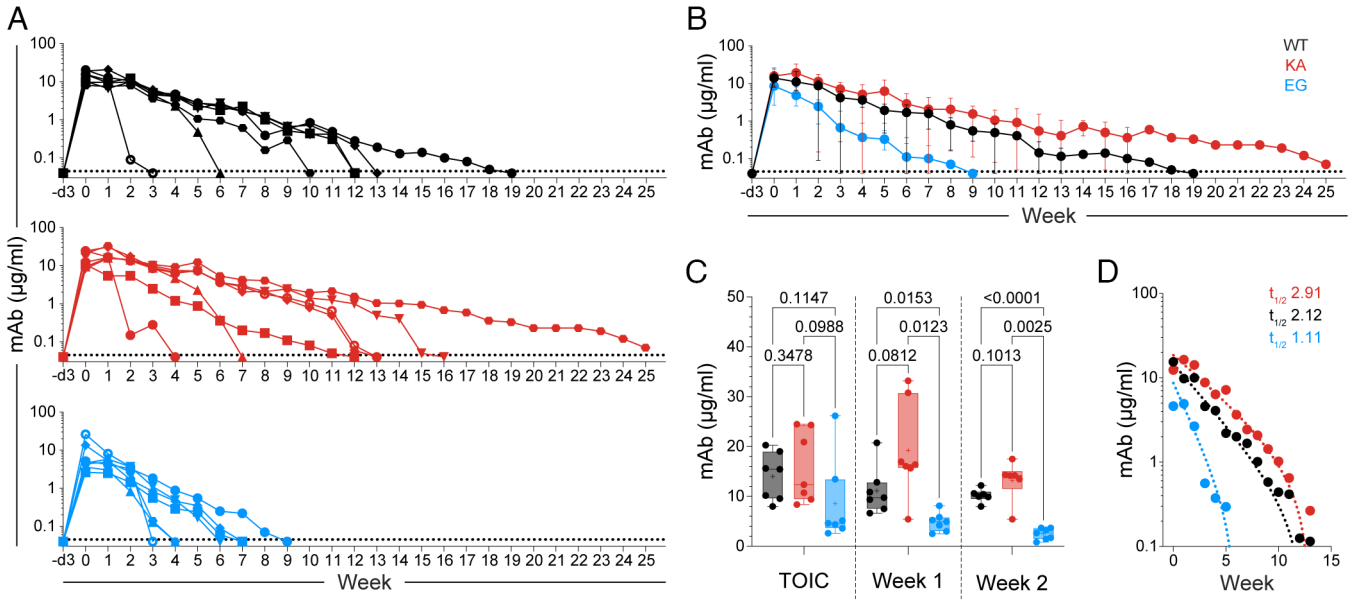

Fig. 3. Fc mutations impacting complement interactions influence mAb pharmacokinetics. (*A* and *B*) Plasma bNAb concentrations observed in individual animals (*A*) and mean and range for each group (*B*) over time. (*C*) Grouped comparison of plasma bNAb concentration detected over the first 3 wk of challenges. Box and whisker plots show range and interquartile range, with median represented by a bar and *P* values from Brown–Forsythe and Welch two-way ANOVA corrected for multiple comparisons by controlling the false discovery rate. (*D*) One-phase decay and slow bNAb half-life ($t_{1/2}$, weeks) in plasma by treatment group.

Results of sera assessment at this time point demonstrated that despite significantly impacted PK, 10-1074.EG-treated animals displayed significantly greater specific SHIV lysis than that of animals treated with either unmodified (P = 0.0072) or 10-1074.KA (P = 0.0012) using autologous serum as a source of complement (Fig. 4*A*). In contrast, both at the initial and following challenge timepoints, the reduced serum levels of 10.1074.EG were associated with reduced neutralization activity relative to unmodified 10-1074 across timepoints ($P \leq 0.0266$) (Fig. 4*B*).

Complement Activity Affects the Level of bNAb Associated with Breakthrough Infection. Given the well-established importance of neutralizing antibody titer to protection (47, 48), it is understood that bNAbs with faster plasma clearance rates will offer less protection against repeat challenges over time. Alternative metrics have been used to benchmark in vivo potency across distinctly designed studies of bNAbs that may naturally exhibit distinct PK profiles (49). Grounded in this analysis, we determined the concentration of bNAb in plasma present at the time of infection/loss of viral suppression (Fig. 4*C*). In this way, a median effective concentration (EC_{50}) of mAb can be established for each treated group. Relative to unmodified 10-1074, the median EC_{50} of 10-1074.EG was improved fivefold (P = 0.048), and that of 10-1074.KA was reduced twofold (P = 0.012) (Fig. 4*D*). Exclusion of subjects with detectable ADA responses resulted in greater confidence in the differences observed between groups (*SI Appendix*, Fig. S3). Thus, more bNAb was required to prevent plasma viremia when complement activity was eliminated, and less bNAb was required to protect animals from infection and/or suppress viremia when complement activity was enhanced.

To further evaluate this observation, we repeated this analysis, comparing the levels of neutralizing activity observed in all animals treated with either unmodified or complement-enhanced 10-1074 (Fig. 5). The median level of neutralizing antibody titers (NT_{50}) observed in animals treated with unmodified 10-1074 were 4.7-fold greater than those observed for 10-1074.EG (P = 0.055) (Fig. 5*A*). Modified Kaplan–Meier curve analysis conditioned on plasma viremia exhibited a similar confidence in the depression of neutralization activity for 10-1074.EG (P = 0.058) observed at breakthrough (Fig. 5*B*). Collectively, this analysis demonstrates that both the levels and neutralizing activity of a bNAb associated with either preventing infection or suppressing systemic viremia can be decreased when complement-mediated effector function activity is enhanced.

Discussion

Early bNAbs provided protection to NHPs against chimeric SHIV challenge, but required high serum titers deemed impractical for translation to human efficacy trials (50–53), motivating discovery of more potent bNAbs (8, 22, 23, 54, 55). Among clinical studies, the AMP efficacy trials of VRC01 represent a milestone in proof of concept for AMP, demonstrating the safety, tolerability, logistical feasibility, and likely protective efficacy of sufficiently potent bNAb PrEP in large and diverse populations of healthy, at-risk individuals (7, 56, 57). However, these studies also made painfully clear that to achieve meaningful efficacy in the field, considerable improvement will be critical to combat the local and global diversity of circulating strains that may resist neutralization by the bNAb being administered.

While evidence that effector function contributes to antiviral activity in vivo based on compromised protection afforded by loss-of-function variants is broad and seen across species (27, 29, 30, 32), it is not universal for all mAbs (37, 38). Despite this established contribution, and numerous supportive results in mouse models for HIV and other pathogens (27, 58–63), improved protection associated with augmented bNAb effector activity has not been observed in the NHP model, where modifications increasing Fc affinity for FcγR or C1q have been associated with reduced mAb half-life (33) and detrimental hyperactivation of effector cells (32).

Because studies in NHP have shown that the importance of effector functions vary among bNAbs, and because the sole NHP experiment probing the contribution complement activation alone was conducted in the context of a bNAb without potent

Downloaded from https://www.pnas.org by INSTITUT PASTEUR MEDIATHEQUE SCIENTIFIC on July 19, 2023 from IP address 157.99.174.25.

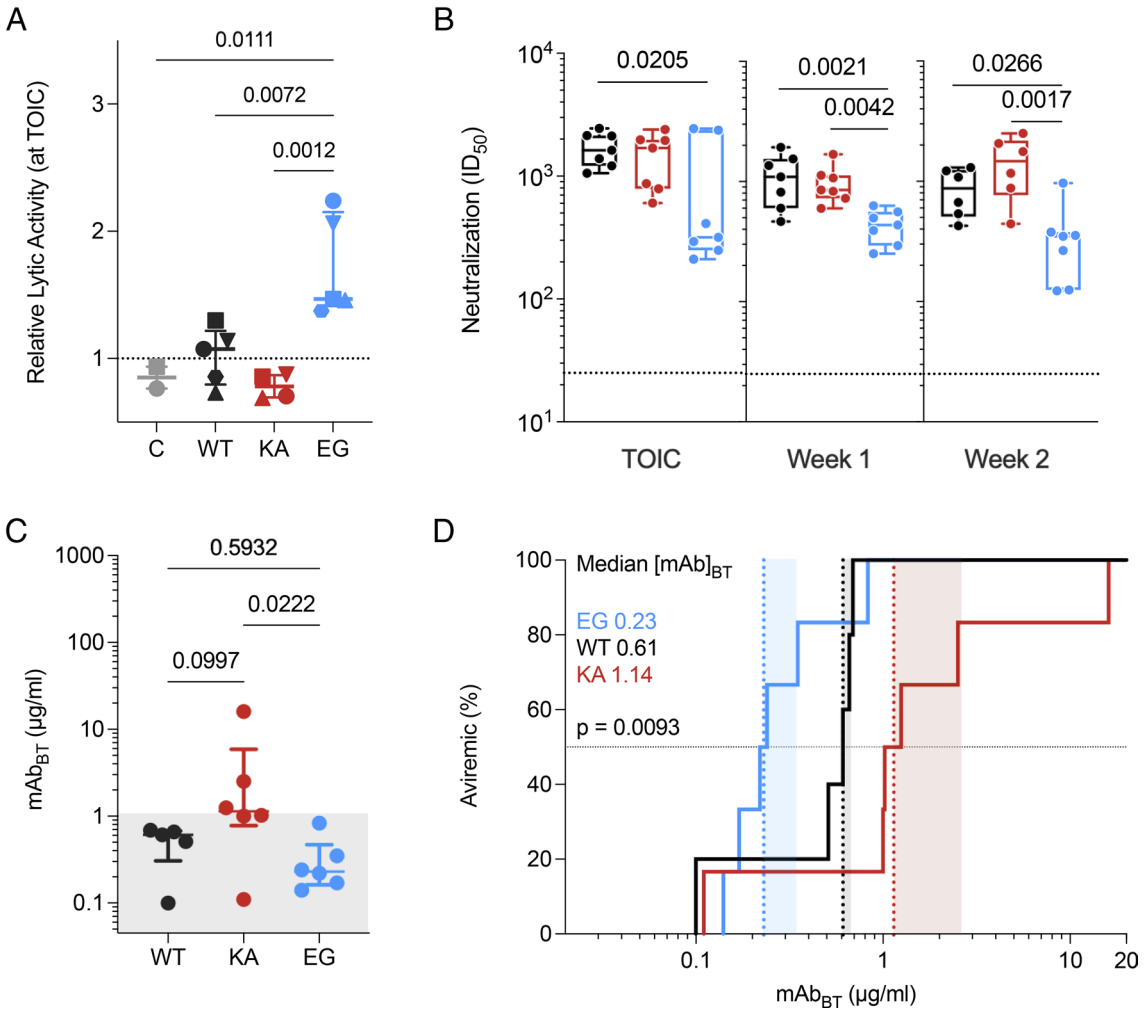

Fig. 4. Complement activation contributes to protection. Greater bnAb concentrations are required to restrict plasma viremia when complement activity is reduced, and lower bnAb concentrations are required to restrict plasma viremia when complement activity is enhanced. (*A*) Relative complement-dependent lytic activity against $SHIV_{SF162P3}$ virions in treated animals. Relative activity was defined as lytic activity in serum 3 d post-mAb treatment at the time of initial challenge (TOIC) normalized to that of serum prior to treatment. Dotted line indicates no change in lytic activity. (*B*) Neutralization titers of plasma samples drawn from mAb treated animals over time. Box and whisker plots depict interquartile range, minimum, mean, and maximum values. Dotted line indicates limit of detection. (*C*) Concentration at breakthrough (mAb_{BT}) by treatment group, with median and interquartile range displayed along with individual animals. Gray region represents the literature-derived value of expected breakthrough for 10.1074, and *P* values from an uncorrected Dunn's test. (*D*) Survival analysis reporting viremia status of each group as a function of plasma antibody concentration. Vertical dotted lines represent median breakthrough concentrations for each group, values reported in the *Inset*. Shaded regions indicate BT_{50}-BT_{80} range. Four ADA-positive animals were excluded from the analysis in *C* and *D* due to undetectable mAb in plasma at the time of breakthrough. Statistical comparisons were performed using an ordinary one-way ANOVA of normalized (*A*) and log-transformed (*B*) values followed by Tukey's post-hoc correction for multiple comparisons. Comparisons in panel (*C*) were conducted using an uncorrected Dunn's test, and survival analysis in panel (*D*) was performed using the log-rank (Mantel–Cox) test. Statistical significance was determined using an alpha level of 0.05 and performed in GraphPad Prism 9.4.1.

complement activity (30, 39, 40), we sought to revisit the contribution of antibody-mediated complement activation on bNAb efficacy using a bNAb with high activity (39, 40). While the role of complement in HIV protection and pathogenesis has been rigorously studied and debated for decades, data present a complicated picture (27, 33, 38, 63–78). Importance is both illustrated and equivocated based on the complement evasion mechanisms that have been developed by the virus (39, 79). Studies have shown that plasma from HIV-infected individuals is capable of lysing and inactivating autologous and heterologous virus in association with reduced viremia (65, 66), and V1-V2-specific complement-activating serum antibody correlated with reduced infection risk in the RV144 vaccine trial (71). In contrast, primary infected cells appear resistant to lysis (39), though it remains unclear whether sublytic complement opsonization imparts in vivo consequences, or whether robust complement-mediated lysis of cell-free virus has a protective impact.

Here, to better investigate the role of complement and its functional augmentation in an NHP model, we subcutaneously delivered a single moderate dose of the unmodified V3 base-directed bNAb, 10-1074 (41), and modified Fc variants EG [E430G (43)) and KA (K322A (42)] that indirectly enhance or directly abrogate complement recruitment, respectively, and subsequently conducted weekly low-dose intrarectal SHIV challenges. Distinctly from other complement-enhancing modifications that directly increase the 1-to-1 affinity between the globular head of C1q and Fc, E430G promotes interaction between the Fcs of adjacent antibodies (43), which is a prerequisite for optimal C1 binding and activation (80–82). Using the robust complement-activating V3-specific bNAb 10-1074, the above attributes make the minimally modified KA and EG variants suitable tools for investigating the specific contribution of complement activation in antibody-mediated prevention of HIV-1 infection.

Downloaded from https://www.pnas.org by INSTITUT PASTEUR MEDIATHEQUE SCIENTIFIC on July 19, 2023 from IP address 157.99.174.25.

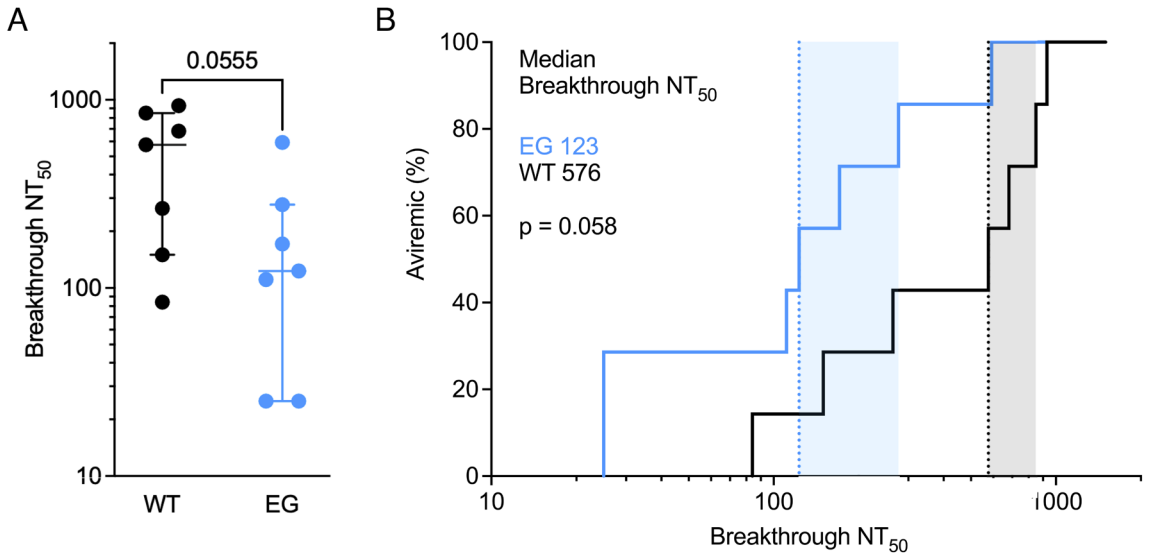

Fig. 5. Increased complement activation decreases the neutralization titer associated with breakthrough plasma viremia. (*A*) Neutralization titer midpoint (NT_{50}) at plasma viremia breakthrough for animals treated with unmodified (WT, black) or enhanced (EG, blue) 10-1074. Bars indicate median and interquartile ranges. (*B*) Survival analysis reporting viremia status of animals treated with unmodified (WT, black) or enhanced (EG, blue) 10-1074 as a function of plasma antibody neutralization activity (NT_{50}) of each group as a function of neutralizing antibody activity observed at breakthrough. Vertical dotted lines represent median breakthrough concentrations for each group, values reported in the *Inset*. Shaded regions indicate breakthrough BT_{50}-BT_{80} range. Comparisons in panel (*A*) were conducted using an uncorrected Dunn's test, and survival analysis in panel (*B*) was performed using the log-rank (Mantel–Cox) test. Statistical significance was determined using an alpha level of 0.05 and performed in GraphPad Prism 9.4.1.

Importantly, these variants significantly impact neither binding to rhesus macaque FcγRs, FcRn, and Env nor in vitro measures of neutralization, ADCC, and ADCP relative to unmodified 10-1074. Overall, we observed no differences in peak PVL or viral setpoint between all groups, nor in the median number of challenges to breakthrough infection between the unmodified 10-1074- and KA- pretreated groups. In contrast, animals receiving the EG variant were protected for only about half as many challenges. However, the PK properties of each 10-1074 variant diverged from the unmodified bNAb in opposing directions, with KA showing moderately improved persistence and EG exhibiting impaired half-life. There is mixed evidence from other studies regarding the impact of Fc modifications developed to alter antibody–FcR interaction profiles on antibody PK. On the one hand, across a range of antibodies with different specificities and both FcR enhancing and abrogating Fc modifications, no dramatic PK differences were reported in cynomolgus monkeys (83). On the other hand, at least two passive immunization studies using FcR-binding-enhanced variants in rhesus macaques have shown considerably impacted PK profiles (32, 33). The E430G variant was selected for this study based on reportedly unaffected clearance rates in a mouse model (43).

Unfortunately, given the dose-dependent nature of antibody activity, bnAb pharmacokinetic profiles can have a considerable influence on the results of traditional time-to-infection analysis. Indeed, the broadening use of Fc domain modifications aimed at extending plasma half-life is motivated by the importance of drug concentration in drug activity. Modified analyses, in which levels of either neutralization activity are analyzed at the time of infection, have been employed to derive in vivo NT_{50} values. Initially used as a means to relate in vitro neutralization potency to in vivo protection across diverse bnAbs and viral strains, we employ this analysis as a means to address in vivo protection in the context of considerable variability in PK. Given the equivalent in vitro neutralization potency of each 10-1074 variant, we expect that if in vivo protection depended only on neutralization, that each variant would exhibit both equivalent neutralization titers and equivalent concentration at infection. Instead, lower levels of drug and lower levels of neutralizing activity were present for the 10-1074 EG variant than those of WT or the KA variant when plasma viremia was detected, suggesting that enhanced complement-dependent effector functions contributed to lowering the threshold of neutralization activity needed to prevent infection.

Our results are subject to several caveats. First, complement activity was not enhanced for the EG variant compared to WT in all functional assays. It is not known which in vitro assay conditions might best reflect relevant conditions in vivo. For example, CDC activity against Env-expressing cells varied by expression level, and which or whether the levels tested best reflect levels present on infected cells is not known. The levels of complement-dependent antibody activity measured in serum, even at the earliest timepoint after administration, were low. While differences in NK cell–mediated cytotoxicity and phagocytosis were not observed, enhanced hexamerization propensity may impact other antibody activities. Additionally, the analysis of protection associated with drug or activity levels rather than the number of challenges may be subject to confounding by variables that were not controlled for in this study. For example, we have presumed that infection occurred at the challenge immediately preceding the time at which plasma viremia was detected and employed serum concentrations or neutralization activity at this timepoint in our analysis. Given the varying PK profiles across antibodies and the potential impact of viremia on antibody levels or their detection, this approach is more conservative than analysis at the time of plasma viremia. However, it is possible that the antibodies tested exhibit different profiles with respect to blocking infection and blocking viral spread, and that our observations reflect differences in the latter as much or more than differences in the former.

Prior studies have shown benefit of Abs engineered for improved effector function in the context of numerous diseases, and these designs are now being investigated clinically. However, the utility of these functionally modified Fc domains has been less clear in primate models. While this lack of evidence may be a simple result of fewer and less well-powered studies, there is some reason to

Downloaded from https://www.pnas.org by INSTITUT PASTEUR MEDIATHEQUE SCIENTIFIC on July 19, 2023 from IP address 157.99.174.25.

think it may reflect differences between models. For example, whereas the antiviral activity of the HIV-specific bNAb PGT121 in preventing the infection of NHP was found to be independent of effector function (37, 38), the ability to restrict infection with pseudovirus in mice has been reported to be dependent on effector function (27). While there are numerous differences beyond host factors between these experiments that could be responsible for this apparent discrepancy, including the Fc domains used to knock down effector function, it is also possible that bnAb-mediated protection is less dependent of effector function in rhesus macaques than that in mice. Which model more faithfully represents the clinic in this regard is unknown.

Prior studies of functionally enhanced bNAbs in primates (32, 33, 48) have not reported enhanced antiviral effects. However, most of these studies have employed antibody variants that, like 10-1074.EG, exhibit more rapid plasma clearance than that of their unmodified counterparts. Here, to reduce the effect of accelerated clearance, an analysis of protection outcomes incorporating median plasma antibody concentrations at the time of breakthrough, supported by a meta-analysis comparing the performance of distinct bNAbs with divergent PK profiles across NHP protection trials with dissimilar protocols (49), was conducted. This analysis yielded the conclusion that the complement knockout variant provided significantly less antiviral activity than that of 10-1074, and that the complement-enhanced variant provided significantly more antiviral activity. These observations support the in vivo contribution of complement to the antiviral activity of an HIV bNAb in primates and demonstrate the ability of an antibody engineered for enhanced effector function to provide enhanced protection in primates. Given ongoing challenges to the development of an efficacious vaccine and observations from the AMP trials that the bar for protection from infection is higher than initially anticipated, means to improve the antiviral activity of bNAbs are of high clinical significance.

Methods

Animals and Virus. Rhesus macaques of Indian origin were cohoused at the Oregon National Primate Research Center and all care and experimental protocols were approved by the Institutional Animal Care and Use Committee at Oregon Health and Science University. Macaques double negative for MHC alleles MamuB*08 and Mamu-B*17 were selected for challenge experiments. Both male and female animals were used in this study. Groups (n = 6 animals for isotype control, n = 7 animals for each 10-1074 variant) were balanced for gender and age. Viral challenges were performed by intrarectal delivery of 1 mL diluted SHIV (ARP-6526, Lot# 170117) corresponding to 30 $TCID_{50}$ in rhesus peripheral blood mononuclear cells (PBMCs).

Affinity to Soluble FcγRs, FcRn, and Env. Generation of recombinant HIV-1_{YU2} gp140 trimer (catalog number ARP-12133) and cloning of 10-1074 variants were documented previously (40). BLI using the Octet RED96 system (Sartorius AG) was used to characterize the 1:1 biophysical interaction between 10-1074 Abs with recombinant rhesus Fc gamma receptors (FcγRIA, FcγRIIA-1, FcγRIIB-1, FcγRIIIA-1) (84), rhesus neonatal Fc receptor (FcRn), and HIV-1_{YU2} gp140 trimer. Measurement of biophysical interactions between the test Abs with low-affinity FcRs and HIV-1 Env was conducted as previously reported (33), with the exception that two-step immobilization was employed using a biotinylated anti-His Ab intermediate. For the measurement of biophysical interaction between the test Abs and FcRn, protocols provided by the manufacturer of biotinylated recombinant rhesus (AcroBiosystems, Cat. #FCM-C82W5) FcRn were followed. Otherwise, all kinetic experiments were performed in freshly prepared and filtered 1× kinetics buffer (1× phosphate-buffered saline [PBS], 0.1% bovine serum albumin [BSA], 0.02% Tween 20, pH 7.4) at 30 °C. Following biosensor activation in wells containing 5 mg/mL biotinylated anti-His tag Ab (catalog number 4603-08; Southern Biotech), loading of His-tagged FcRs or Env to a threshold RU (response units) of 0.3 nm high-precision streptavidin biosensors (catalog number 18-5117; Sartorius AG) was performed. Then, following a 60-s baseline step in kinetics buffer, the loaded biosensors were dipped into twofold serially diluted Ab samples (46.88 to 3000 nM for low-affinity FcRs; 7.84 to 500 nM for FcRn; 0.98 to 62.5 nM for FcγRIA; 0.08 to 60 nM for Env) for a 60-s association step (300-s for Env) and subsequently for 60 s (300-s for Env) in kinetics buffer to measure dissociation. Immobilized receptors were regenerated between Ab analytes by dipping 3 × 5-s into regeneration buffer (10 mM Glycine, pH 1.7). To determine kinetic constants, binding sensorgrams were aligned to the beginning of the association step for interstep correction and Y-aligned to the preassociation baseline step, and following single-reference subtraction consisting of immobilized receptor dipped into kinetics buffer, the processed sensorgrams were globally fit to a 1:1 binding isotherm on ForteBio HT Analysis Software (version 11.1.1.39). For FcRn and FcγRIA, two experiments using streptavidin-coated biosensors (Sartorius AG, Item #18-5019) were conducted to account for variability between the sets of biosensors.

Neutralization. Neutralization was assessed in TZM-bl cells expressing luciferase under the control of the HIV tat promoter as standardized by Wei et al. and clinically validated by Corey et al. using replication-competent $SHIV_{ipd3N4}$ and $SHIV_{SF162P3}$ stocks expanded in CD4-enriched rhesus splenocytes (7, 85), as well as $SHIV_{SF162P3}$ and $SHIV_{AD8\text{-}EO}$ pseudoviruses. Briefly, threefold serial dilutions of Ab were incubated in 150 μL with the indicated virus for 1 h in cDMEM (DMEM [Gibco] supplemented with 4.5 g/L D-glucose, 10% heat-inactivated FBS, 1% L-glutamine, 1% penicillin, and 1% streptomycin) at 37 °C and 5% CO_2. Next, 1×10^4 cells/well were added in 50 μL media further supplemented with 7.5 μg/mL DEAE-dextran to aid viral entry. After 24 h coincubation, 140 μL of media was gently removed from each well and adherent cells were lysed by the addition of 60 μL Bright-Glo (Promega) for 2 min. Eighty microliters was then transferred to black plates and viral infection was determined as the relative level of luciferase activity measured on a Victor X Light plate reader (Perkin Elmer). Repeat measures represent values obtained on separate days by distinct operators and the percent neutralizing activity was calculated using the following formula: [mean no Ab (i.e., virus and cells minus cells-only background)–mean sample (i.e., sample value minus cells-only background)]/[mean no Ab] × 100. Isotype and positive control Abs were included on all assay runs.

ADCP. The phagocytic potential of 10-1074 and the Fc point variants was assessed by a method adapted from Ackerman et al. (86). Fluorescent antigen beads were prepared by conjugating either HIV-1_{BaL} gp120 or HIV-1_{SF162} gp140 trimer (catalog number ARP-12026) to carboxylate-modified yellow-green fluorescent polystyrene beads (ThermoFisher Scientific, F8823) and were confirmed to be properly functionalized by assessing staining using a number of Env-specific mAbs alongside a negative isotype control. To measure ADCP, 10-1074 variants were serially diluted threefold (for $gp120_{BaL}$, 16.67 to 0.62 nM; for $gp140_{SF162}$, 2.5 to 0.04 nM) and mixed with a homogenous solution of a 1:15 ratio of rhesus macaque PBMC effectors to target fluorescent antigen beads. Following a 4 h incubation at 37 °C and 5% CO_2, the sampled contents of each well were analyzed by flow cytometry on a MACSQuant Analyzer 10 system (Miltenyi Biotec), and ADCP results were reported as a phagocytosis score (P score) metric [P score = (% PBMCs that engulfed at least one fluorescent bead or the percentage of gated effector cells with FITC signal above a threshold MFI) * (the average number of beads engulfed or the MFI signal of the FITC+ gated effectors)].

ADCC. Assessment of ADCC activity was performed as described previously (87). In brief, CD4+CCR5+ NKR24 target cells expressing luciferase under tat-dependent promoter control were infected with replication-competent $SHIV_{SF162P3}$ (200 ng/mL p27) by spinoculation at 1,200 × g for 2 h with 40 μg/mL polybrene. Three days later, 1×10^4 target cells/well were coincubated with CD16-expressing effector NK cell line (KHYG-1) at an effector-to-target ratio of 10:1 with or without serial Ab dilutions in 200 μL assay media (RPMI supplemented with 5 U/ ml IL-2) in round-bottom 96-well plates at 37 °C and 5% CO_2. Antibodies and plasma dilutions were plated in duplicate. After 8 h coincubation, each assay well was mixed by pipetting and 150 μL transferred to black flat-bottom plates containing 50 μL Bright-Glo (Promega) and incubated for 2 min at 25 °C. Luminescence was measured on a Victor X Light plate reader (Perkin Elmer), and relative light units (RLU) were normalized according to the following formula: [sample mean–background (mock-infected targets and effectors)]/[maximum (SHIV-infected targets and effectors, no mAb–background)] × 100. ADCC activity is reported as the percentage loss of RLU.

Downloaded from https://www.pnas.org by INSTITUT PASTEUR MEDIATHEQUE SCIENTIFIC on July 19, 2023 from IP address 157.99.174.25.

C1q Binding to Beads. Analytical flow cytometry was used to assess the ability of the 10-1074 panel to recruit rhesus macaque C1q to the surface of antigen-conjugated beads. Antigen beads were prepared by covalently coupling HIV-1_{SF162} gp120 and HIV-1_{YU2} gp140 trimer to coded MagPlex® superparamagnetic carboxylated magnetic microparticles (Luminex Corp.) using carbodiimide cross-linking chemistry as previously described (88). To carry out the C1q binding assay, antigen-coated beads were incubated with serially diluted Ab (fivefold, 0.63 to 100 nM) for 1 h at room temperature followed by the addition of individual rhesus macaque serum (Oregon National Primate Research Center) at a final concentration of 1:12,500 and incubated overnight at 4 °C. Following washing, samples were incubated with 0.1 μg/well (1.0 μg/mL) biotin anti-human C1q (CL7611B, Cedarlane) for 1 h at RT with shaking. Following washes, the bound anti-huC1q reagent was detected by resuspension in streptavidin-phycoerythrin (PJRS25, ProZyme) at 1:500 for 30 min at RT and washed, and data reported as median fluorescent intensity (MFI) were acquired on the FLEXMAP 3D® system (Luminex Corp.). Data shown are representative of at least two independent experiments. Assay wells containing assay buffer in lieu of antibody were used to assess background, nonantibody-dependent C1q association with antigen-conjugated beads.

SHIV Lysis. The ability for each mAb, or complement-preserved serum from mAb-treated rhesus macaques, to mediate complement lysis of cell-free replication-competent challenge virus, $SHIV_{SF162P3}$, was assessed by the measurement of capsid protein p27, released into the supernatant following viral membrane disruption as previously described (33, 89). In a black 96-well clear flat-bottom plate (655906, Greiner Bio-One), a final concentration of 0.2 ng/mL [p27] of $SHIV_{SF162P3}$ virus was mixed with either 1:100 final concentration of complement-preserved rhesus macaque serum (n = 5 individuals) or heat-inactivated rhesus serum, or an equivalent volume of disruption buffer for the standard curve and 100% lysis control. Assessment of plasma SHIV ADCML involved coincubation of complement-preserved macaque serum from pretreated and "week 0" (containing ~peak [bNAb]) timepoints with challenge virus. Heat-inactivated complement serum (56 °C, 30 min) and wells containing active complement serum without antibody served as negative controls for baseline p27 concentrations and complement-mediated lysis via antibody-independent pathways, respectively. The plates were incubated at 37 °C gentle shaking (400 RPM), and after 30 min, 10 μL anti-p27 capture beads were spiked into each well and placed at 37 °C for another 30 min with gentle shaking. Following the complete hour, the plate was placed on ice to halt the reaction. Quantification of the released p27 was carried out using a bead-based sandwich assay. Briefly, MagPlex® beads preconjugated to an anti-SIVmac251 p27 monoclonal antibody (ARP-13443, HIV Reagent Program) were incubated with each sample for 1 h at RT with gentle orbital shaking, followed by washing on an automated plate washer. The degree of p27 bound to the beads was detected via incubation with 1.0 μg/mL biotin-anti-SIVmac p27 (ARP-1610, HIV Reagent Program) for 1 h at room temperature with shaking and subsequent staining with 1:200 streptavidin-phycoerythrin (PJRS25, ProZyme). After incubation and washing steps, the beads were resuspended in xMAP® sheath fluid (Luminex Corp), and MFI values were recorded by the MAGPIX® System (Luminex Corp). Data were reported as mean and SD of three technical replicates and are representative of at least two independent experiments.

Complement-Dependent Cytolysis. Cells (1×10^5) expressing varying levels of Env (39) were cultivated in the presence of 50% human or macaque serum and with or without antibodies (15 μg mL^{-1}). To measure cell death, the live/dead fixable aqua dead cell marker (1:1,000 in PBS; Life Technologies) was added for 30 min at 4 °C before fixation with PFA 4%. Data were acquired on an Attune Nxt (Life Technologies) flow cytometer and analyzed using FlowJo software. CDC was calculated using the following formula: 100 × (% of dead cells with antibody − % of dead cells without antibody)/(100 − % of dead cells without antibody). Negative values were set to zero.

Quantification of PVL. PVLs were determined by quantifying SIVgag vRNA from nucleic acid in plasma by quantitative reverse transcription-PCR (RT-PCR) as detailed previously (90). In brief, 2 μg nucleic acid was amplified for 45 cycles in 30 μL Fast Advanced MasterMix on a QuantStudio 6 Flex instrument (Applied Biosystems, Life Technologies), and virus copy numbers were estimated by interpolation from a pBSII-SIVgag standard curve. The following primers and probe were used for all protocols to amplify and detect a conserved region in SIVgag: SGAG21 forward primer (GTCTGCGTCATPTGGTGCATTC), SGAG22 reverse primer (CACTAGKT GTCTCTGCACTATPTGTTTTG), and pSGAG23 probe (5′-6-carboxyfluorescein [FAM]-CTTCPTCAGTKTGTTTCACTTTCTCTTCTGCG-black hole quencher [BHQ1]-3′).

Detection of Plasma Antibody. The determination of detectable plasma antibody concentrations was carried out by ELISA and performed largely as described by Spencer et al. (33). Plates were coated with 10-1074 anti-idiotype mAb (DHVI Protein Production Facility) for detection of 10-1074 mAb, or with 10-1074 and variants for measuring ADA. Flat-bottom plates were coated with the antigen of interest by incubating 0.5 to 1 μg/mL in 0.2M H_2CO_3 buffer pH 9.4 at 4 °C overnight. The plates were then washed in binding buffer (PBS pH 7.4 + 0.1% Triton X-100) and blocked with 150 μL PBS containing 5% dried milk and 1% goat serum for 1 h at room temperature. Blocking buffer was discarded and threefold serial dilutions of plasma or mAb were added to unwashed cells in 50 μL binding buffer. After 1 h at room temperature, the plates were washed 3× and then incubated for 1 additional hour with 50 μL 1:5,000 dilution of goat anti-human H&L (assays 1 to 3) or 50 μL 1:3,000 dilution of mouse anti-macaque IgG mAb 1B3 (assay 4) conjugated to horse radish peroxidase (from Invitrogen and NIH AIDS Reagents program, respectively). The plates were then washed 5×, and the bound Ab was visualized by the addition of 50 μL tetramethylbenzidine (Southern Biotech) for 10 min before stopping the reaction with 50 μL 1N H_2SO_4. Optical density was immediately quantified on a SoftMax® Pro 5 microplate reader (Molecular Devices) at 450 nm.

Statistical Analysis. Statistical analysis was performed as indicated in the figure legends. Comparisons were performed using one-way ANOVA (corrected for multiple comparisons) using either a nonparametric Friedman test, uncorrected Dunn's test, Tukey's post-hoc correction for multiple comparisons, or one-way ANOVAs with the Geisser–Greenhouse correction and Holm–Šidák correction for multiple comparisons in Figs. 1 *G* and *H*, 2 *C*–*E*, and 4*C*. For survival analysis in Figs. 2*C* and 4*D* and *SI Appendix*, Fig. S1 *D* and *E*, statistical comparisons were performed using the log-rank (Mantel–Cox) test with *P* values for significant relationships shown from Fisher's LSD tests. As shown in Fig. 3 *C* and *D*, the Brown–Forsythe and Welch two-way ANOVA corrected for multiple comparisons by controlling the false discovery rate and a one-phase decay and slow bNAb half-life (t1/2, weeks) were used to compare groups. PVLs were presented and analyzed using log_{10}-transformed data. Statistical significance was determined using an alpha level of 0.05 and performed in GraphPad Prism 9.4.1.

Data, Materials, and Software Availability. All study data are available in the article and/or *SI Appendix*.

ACKNOWLEDGMENTS. We thank Diane Kubitz and Jonathan Otsuji at The Scripps Research Institute antibody production core facility for monoclonal antibody production, Christina Corbaci for assistance with figure design and production, David Evans for providing the $CD4^+CCR5^+$ NKR24 and KHYG-1 NK cell lines, Rockefeller University for the expression plasmid for 10-1074, and Duke University DHVI Protein Production Facility for the 10-1074 anti-idiotype antibody. We acknowledge the NIH AIDS Reagent Program for providing the following reagents: TZM-bl cells (ARP-11796) and $SHIV_{SF162P3}$ virus stock (ARP-6526), vector pcDNA3.1 containing HIV-1, strain YU2 gp140Δ683(-/GCN4) in pcDNA3.1, ARP-12133, contributed by Dr. Joseph Sodroski, and HIV type 1 SF162 gp140 trimer protein, recombinant from HEK293T cells, ARP-12026, contributed by Dr. Leo Stamatatos. This work was supported by the following grants: R01 AI129801, P51 OD011092, R01 AI131975, and U42 OD023038-03.

Author affiliations: [a]Thayer School of Engineering, Dartmouth College, Hanover, NH 03755; [b]Division of Pathobiology and Immunology, Oregon National Primate Research Center, Oregon Health and Science University, Beaverton, OR 97006; [c]Biostatistics Shared Resources, Knight Cancer Institute, Oregon Health and Science University, Portland, OR 97239; [d]Biostatistics & Bioinformatics Core, Oregon National Primate Research Center, Oregon Health & Science University, Beaverton, OR 97006; [e]Institut Pasteur, Université de Paris, CNRS UMR3569, Virus and Immunity Unit, 75015 Paris, France; [f]Université de Paris, École doctorale BioSPC 562, 75013 Paris, France; [g]Vaccine Research Institute, 94000 Créteil, France; and [h]Department of Microbiology and Immunology, Geisel School of Medicine, Dartmouth College, Hanover, NH 03755

Author contributions: D.A.S., M.E.A., and A.J.H. designed research; B.S.G., D.A.S., S.P., T.O., P.B., J.D., and T.B. performed research; O.S. contributed new reagents/analytic tools; B.S.G., D.A.S., S.P., T.O., P.B., Y.Y., L.G., J.D., T.B., M.E.A., and A.J.H. analyzed data; T.B. contributed to manuscript review; O.S. supervised research and contributed to data and manuscript review; and B.S.G., M.E.A., and A.J.H. wrote the paper.

Downloaded from https://www.pnas.org by INSTITUT PASTEUR MEDIATHEQUE SCIENTIFIC on July 19, 2023 from IP address 157.99.174.25.

1. H. Gruell, F. Klein, Antibody-mediated prevention and treatment of HIV-1 infection. *Retrovirology* **15**, 73 (2018).
2. M. Caskey, F. Klein, M. C. Nussenzweig, Broadly neutralizing anti-HIV-1 monoclonal antibodies in the clinic. *Nat. Med.* **25**, 547–553 (2019).
3. H. Gruell, P. Schommers, Broadly neutralizing antibodies against HIV-1 and concepts for application. *Curr. Opin. Virol.* **54**, 101211 (2022).
4. S. T. Karuna, L. Corey, Broadly neutralizing antibodies for HIV prevention. *Annu. Rev. Med.* **71**, 329–346 (2020).
5. M. D. Miner, L. Corey, D. Montefiori, Broadly neutralizing monoclonal antibodies for HIV prevention. *J. Int. AIDS Soc.* **24**, e25829 (2021).
6. S. R. Walsh, M. S. Seaman, Broadly neutralizing antibodies for HIV-1 prevention. *Front. Immunol.* **12**, 712122 (2021).
7. L. Corey *et al.*, Two randomized trials of neutralizing antibodies to prevent HIV-1 acquisition. *N. Engl. J. Med.* **384**, 1003–1014 (2021).
8. T. Schoofs *et al.*, Broad and potent neutralizing antibodies recognize the silent face of the HIV envelope. *Immunity* **50**, 1513–1529.e9 (2019).
9. P. Schommers *et al.*, Restriction of HIV-1 escape by a highly broad and potent neutralizing antibody. *Cell* **180**, 471–489.e22 (2020).
10. E. D. Rossignol *et al.*, Mining HIV controllers for broad and functional antibodies to recognize and eliminate HIV-infected cells. *Cell Rep.* **35**, 109167 (2021).
11. J. R. Dhande, R. D. Bagul, M. R. Thakar, HIV-gp140-specific antibodies generated from Indian long-term non-progressors mediate potent ADCC activity and effectively lyse reactivated HIV reservoir. *Front. Immunol.* **13**, 844610 (2022).
12. M. Raghavan, V. R. Bonagura, S. L. Morrison, P. J. Bjorkman, Analysis of the pH dependence of the neonatal Fc receptor/immunoglobulin G interaction using antibody and receptor variants. *Biochemistry* **34**, 14649–14657 (1995).
13. D. C. Roopenian *et al.*, The MHC class I-like IgG receptor controls perinatal IgG transport, IgG homeostasis, and fate of IgG-Fc-coupled drugs. *J. Immunol.* **170**, 3528–3533 (2003).
14. J. Zalevsky *et al.*, Enhanced antibody half-life improves in vivo activity. *Nat. Biotechnol.* **28**, 157–159 (2010).
15. S. Y. Ko *et al.*, Enhanced neonatal Fc receptor function improves protection against primate SHIV infection. *Nature* **514**, 642–645 (2014).
16. M. R. Gaudinski *et al.*, Safety and pharmacokinetics of broadly neutralising human monoclonal antibody VRC07-523LS in healthy adults: A phase 1 dose-escalation clinical trial. *Lancet HIV* **6**, e667–e679 (2019).
17. S. Mahomed *et al.*, Safety and pharmacokinetics of monoclonal antibodies VRC07-523LS and PGT121 administered subcutaneously for human immunodeficiency virus prevention. *J. Infect. Dis.* **226**, 510–520 (2022).
18. J. P. Casazza *et al.*, Safety and tolerability of AAV8 delivery of a broadly neutralizing antibody in adults living with HIV: A phase 1, dose-escalation trial. *Nat. Med.* **28**, 1022–1030 (2022).
19. R. S. Rudicell *et al.*, Enhanced potency of a broadly neutralizing HIV-1 antibody in vitro improves protection against lentiviral infection in vivo. *J. Virol.* **88**, 12669–12682 (2014).
20. C. S. Pace *et al.*, Bispecific antibodies directed to CD4 domain 2 and HIV envelope exhibit exceptional breadth and picomolar potency against HIV-1. *Proc. Natl. Acad. Sci. U.S.A.* **110**, 13540–13545 (2013).
21. S. Bournazos, A. Gazumyan, M. S. Seaman, M. C. Nussenzweig, J. V. Ravetch, Bispecific anti-HIV-1 antibodies with enhanced breadth and potency. *Cell* **165**, 1609–1620 (2016).
22. B. Julg *et al.*, Protection against a mixed SHIV challenge by a broadly neutralizing antibody cocktail. *Sci. Transl. Med.* **9**, eaao4235 (2017).
23. R. Gautam *et al.*, A single injection of crystallizable fragment domain–modified antibodies elicits durable protection from SHIV infection. *Nat. Med.* **24**, 610–616 (2018).
24. N. N. Padte, J. Yu, Y. Huang, D. D. Ho, Engineering multi-specific antibodies against HIV-1. *Retrovirology* **15**, 60 (2018).
25. A. Pegu *et al.*, Potent anti-viral activity of a trispecific HIV neutralizing antibody in SHIV-infected monkeys. *Cell Rep.* **38**, 110199 (2022).
26. B. Moldt *et al.*, A nonfucosylated variant of the anti-HIV-1 monoclonal antibody b12 has enhanced FcγRIIIa-mediated antiviral activity in vitro but does not improve protection against mucosal SHIV challenge in macaques. *J. Virol.* **86**, 6189–6196 (2012).
27. S. Bournazos *et al.*, Broadly neutralizing anti-HIV-1 antibodies require Fc effector functions for in vivo activity. *Cell* **158**, 1243–1253 (2014).
28. C. L. Lu *et al.*, Enhanced clearance of HIV-1-infected cells by broadly neutralizing antibodies against HIV-1 in vivo. *Science* **352**, 1001–1004 (2016).
29. P. Wang *et al.*, Quantifying the contribution of Fc-mediated effector functions to the antiviral activity of anti–HIV-1 IgG1 antibodies in vivo. *Proc. Natl. Acad. Sci. U.S.A.* **117**, 18002–18009 (2020).
30. A. J. Hessell *et al.*, Fc receptor but not complement binding is important in antibody protection against HIV. *Nature* **449**, 101–104 (2007).
31. A. J. Hessell *et al.*, Broadly neutralizing human anti-HIV antibody 2G12 is effective in protection against mucosal SHIV challenge even at low serum neutralizing titers. *PLoS Pathog.* **5**, e1000433 (2009).
32. M. Asokan *et al.*, Fc-mediated effector function contributes to the in vivo antiviral effect of an HIV neutralizing antibody. *Proc. Natl. Acad. Sci. U.S.A.* **117**, 18754–18763 (2020).
33. D. A. Spencer *et al.*, Phagocytosis by an HIV antibody is associated with reduced viremia irrespective of enhanced complement lysis. *Nat. Commun.* **13**, 662 (2022).
34. C. E. Hioe *et al.*, Non-neutralizing antibodies targeting the immunogenic regions of HIV-1 envelope reduce mucosal infection and virus burden in humanized mice. *PLoS Pathog.* **18**, e1010183 (2022).
35. A. J. Hessell *et al.*, Effective, low-titer antibody protection against low-dose repeated mucosal SHIV challenge in macaques. *Nat. Med.* **15**, 951–954 (2009).
36. M. S. Parsons, A. W. Chung, S. J. Kent, Importance of Fc-mediated functions of anti-HIV-1 broadly neutralizing antibodies. *Retrovirology* **15**, 58 (2018).
37. M. S. Parsons *et al.*, Fc-dependent functions are redundant to efficacy of anti-HIV antibody PGT121 in macaques. *J. Clin. Invest.* **129**, 182–191 (2018).
38. L. Hangartner *et al.*, Effector function does not contribute to protection from virus challenge by a highly potent HIV broadly neutralizing antibody in nonhuman primates. *Sci. Transl. Med.* **13**, eabe3349 (2021).
39. J. Dufloo *et al.*, Anti-HIV-1 antibodies trigger non-lytic complement deposition on infected cells. *EMBO Rep.* **21**, e49351. (2020).
40. B. S. Goldberg *et al.*, Revisiting an IgG Fc loss-of-function experiment: The role of complement in HIV broadly neutralizing antibody b12 activity. *mBio* **12**, e0174321 (2021).
41. H. Mouquet *et al.*, Complex-type N-glycan recognition by potent broadly neutralizing HIV antibodies. *Proc. Natl. Acad. Sci. U.S.A.* **109**, E3268–E3277 (2012).
42. E. E. Idusogie *et al.*, Mapping of the C1q binding site on rituxan, a chimeric antibody with a human IgG1 Fc. *J. Immunol.* **164**, 4178–4184 (2000).
43. R. N. de Jong *et al.*, A novel platform for the potentiation of therapeutic antibodies based on antigen-dependent formation of IgG hexamers at the cell surface. *PLoS Biol.* **14**, e1002344 (2016).
44. B. E. De Goeij *et al.*, Hexabody-CD38, a novel CD38 antibody with a hexamerization enhancing mutation, demonstrates enhanced complement-dependent cytotoxicity and shows potent anti-tumor activity in preclinical models of hematological malignancies. *Blood* **134**, 3106 (2019).
45. S. C. Oostindie *et al.*, DuoHexaBody-CD37®, a novel biparatopic CD37 antibody with enhanced Fc-mediated hexamerization as a potential therapy for B-cell malignancies. *Blood Cancer J.* **10**, 1–13 (2020).
46. R. D. Astronomo *et al.*, Neutralization takes precedence over IgG or IgA isotype-related functions in mucosal HIV-1 antibody-mediated protection. *EBioMedicine* **14**, 97–111 (2016).
47. R. Willey, M. C. Nason, Y. Nishimura, D. A. Follmann, M. A. Martin, Neutralizing antibody titers conferring protection to Macaques from a Simian/human immunodeficiency virus challenge using the TZM-bl assay. *AIDS Res. Hum. Retroviruses* **26**, 89–98 (2010).
48. B. Moldt *et al.*, Highly potent HIV-specific antibody neutralization in vitro translates into effective protection against mucosal SHIV challenge in vivo. *Proc. Natl. Acad. Sci. U.S.A.* **109**, 18921–18925 (2012).
49. A. Pegu *et al.*, A meta-analysis of passive immunization studies shows that serum-neutralizing antibody titer associates with protection against SHIV challenge. *Cell Host Microbe* **26**, 336–346.e3 (2019).
50. E. A. Emini *et al.*, Prevention of HIV-1 infection in chimpanzees by gpl20 V3 domain-specific monoclonal antibody. *Nature* **355**, 728–730 (1992).
51. J. R. Mascola *et al.*, Protection of Macaques against pathogenic simian/human immunodeficiency virus 89.6PD by passive transfer of neutralizing antibodies. *J. Virol.* **73**, 4009–4018 (1999).
52. J. R. Mascola *et al.*, Protection of macaques against vaginal transmission of a pathogenic HIV-1/SIV chimeric virus by passive infusion of neutralizing antibodies. *Nat. Med.* **6**, 207–210 (2000).
53. T. W. Baba *et al.*, Human neutralizing monoclonal antibodies of the IgG1 subtype protect against mucosal simian-human immunodeficiency virus infection. *Nat. Med.* **6**, 200–206 (2000).
54. B. Julg *et al.*, Broadly neutralizing antibodies targeting the HIV-1 envelope V2 apex confer robust protection against a clade C SHIV challenge. *Sci. Transl. Med.* **9**, eaal1321 (2017).
55. B. Julg *et al.*, Protective efficacy of broadly neutralizing antibodies with incomplete neutralization activity against Simian-Human immunodeficiency virus in Rhesus monkeys. *J. Virol.* **91**, e01187-17 (2017).
56. S. Takuva *et al.*, Infusion reactions after receiving the broadly neutralizing antibody VRC01 or placebo to reduce HIV-1 acquisition: Results from the phase 2b antibody-mediated prevention randomized trials. *J. Acquir. Immune Defic. Syndr.* **89**, 405–413 (2022).
57. P. B. Gilbert *et al.*, Neutralization titer biomarker for antibody-mediated prevention of HIV-1 acquisition. *Nat. Med.* **28**, 1924–1932 (2022).
58. S. Bournazos, D. J. DiLillo, A. J. Goff, P. J. Glass, J. V. Ravetch, Differential requirements for FcγR engagement by protective antibodies against Ebola virus. *Proc. Natl. Acad. Sci. U.S.A.* **116**, 20054–20062 (2019).
59. S. Bournazos, D. Corti, H. W. Virgin, J. V. Ravetch, Fc-optimized antibodies elicit CD8 immunity to viral respiratory infection. *Nature* **588**, 485–490 (2020).
60. B. M. Gunn *et al.*, A role for fc function in therapeutic monoclonal antibody-mediated protection against Ebola virus. *Cell Host Microbe* **24**, 221–233.e5 (2018).
61. B. M. Gunn, S. Bai, Building a better antibody through the Fc: Advances and challenges in harnessing antibody Fc effector functions for antiviral protection. *Hum. Vaccin. Immunother.* **17**, 4328–4344 (2021).
62. N. A. Pereira, K. F. Chan, P. C. Lin, Z. Song, The "less-is-more" in therapeutic antibodies: Afucosylated anti-cancer antibodies with enhanced antibody-dependent cellular cytotoxicity. *MAbs* **10**, 693–711 (2018).
63. T. Li *et al.*, Modulating IgG effector function by Fc glycan engineering. *Proc. Natl. Acad. Sci. U.S.A.* **114**, 3485–3490 (2017).
64. W. E. Robinson *et al.*, Human monoclonal antibodies to the human immunodeficiency virus type 1 (HIV-1) transmembrane glycoprotein gp41 enhance HIV-1 infection in vitro. *Proc. Natl. Acad. Sci. U.S.A.* **87**, 3185–3189 (1990).
65. M. M. I. Aasa-Chapman *et al.*, Detection of antibody-dependent complement-mediated inactivation of both autologous and heterologous virus in primary human immunodeficiency virus type 1 infection. *J. Virol.* **79**, 2823–2830 (2005).
66. M. Huber *et al.*, Complement lysis activity in autologous plasma is associated with lower viral loads during the acute phase of HIV-1 infection. *PLoS Med.* **3**, e441 (2006).
67. H. Stoiber, Z. Banki, D. Wilflingseder, M. P. Dierich, Complement-HIV interactions during all steps of viral pathogenesis. *Vaccine* **26**, 3046–3054 (2008).
68. Q. Yu, R. Yu, X. Qin, The good and evil of complement activation in HIV-1 infection. *Cell Mol. Immunol.* **7**, 334–340 (2010).
69. B. A. Heesters *et al.*, Follicular dendritic cells retain infectious HIV in cycling endosomes. *PLoS Pathog.* **11**, e1005285 (2015).
70. R. Herrero *et al.*, Association of complement receptor 2 polymorphisms with innate resistance to HIV-1 infection. *Genes Immun.* **16**, 134–141 (2015).
71. L. G. Perez *et al.*, V1V2-specific complement activating serum IgG as a correlate of reduced HIV-1 infection risk in RV144. *PLoS One* **12**, e0180720 (2017).
72. G. Lofano *et al.*, Antigen-specific antibody Fc glycosylation enhances humoral immunity via the recruitment of complement. *Sci. Immunol.* **3**, eaat7796 (2018).
73. S. I. Richardson *et al.*, HIV-specific Fc effector function early in infection predicts the development of broadly neutralizing antibodies. *PLoS Pathog.* **14**, e1006987 (2018).
74. G. Meza *et al.*, Association of complement C3d receptor 2 genotypes with the acquisition of HIV infection in a trial of recombinant glycoprotein 120 vaccine. *AIDS* **34**, 25–32 (2020).
75. P. Bhattacharya *et al.*, Complement opsonization of HIV affects primary infection of human colorectal mucosa and subsequent activation of T cells. *Elife* **9**, e57869 (2020).
76. C. Serrano-Rísquez *et al.*, CD46 genetic variability and HIV-1 infection susceptibility. *Cells* **10**, 3094 (2021).

Downloaded from https://www.pnas.org by INSTITUT PASTEUR MEDIATHEQUE SCIENTIFIC on July 19, 2023 from IP address 157.99.174.25.

77. C. Svanberg *et al.*, Complement-opsonized HIV modulates pathways involved in infection of cervical mucosal tissues: A transcriptomic and proteomic study. *Front. Immunol.* **12**, 625649 (2021).
78. W. Posch *et al.*, Complement potentiates immune sensing of HIV-1 and early type I interferon responses. *mBio* **12**, e0240821 (2021).
79. M. Saifuddin *et al.*, Role of virion-associated glycosylphosphatidylinositol-linked proteins CD55 and CD59 in complement resistance of cell line-derived and primary isolates of HIV-1. *J. Exp. Med.* **182**, 501–509 (1995).
80. C. A. Diebolder *et al.*, Complement is activated by IgG hexamers assembled at the cell surface. *Science* **343**, 1260–1263 (2014).
81. G. Wang *et al.*, Molecular basis of assembly and activation of complement component C1 in complex with immunoglobulin G1 and antigen. *Mol. Cell* **63**, 135–145 (2016).
82. D. Ugurlar *et al.*, Structures of C1-IgG1 provide insights into how danger pattern recognition activates complement. *Science* **359**, 794–797 (2018).
83. M. K. Leabman *et al.*, Effects of altered FcγR binding on antibody pharmacokinetics in cynomolgus monkeys. *MAbs* **5**, 896–903 (2013).
84. Y. N. Chan *et al.*, IgG binding characteristics of Rhesus Macaque FcγR. *J. Immunol.* **197**, 2936–2947 (2016).
85. X. Wei *et al.*, Antibody neutralization and escape by HIV-1. *Nature* **422**, 307–312 (2003).
86. M. E. Ackerman *et al.*, A robust, high-throughput assay to determine the phagocytic activity of clinical antibody samples. *J. Immunol. Methods* **366**, 8–19 (2011).
87. M. D. Alpert *et al.*, A novel assay for antibody-dependent cell-mediated cytotoxicity against HIV-1- or SIV-infected cells reveals incomplete overlap with antibodies measured by neutralization and binding assays. *J. Virol.* **86**, 12039–12052 (2012).
88. E. P. Brown *et al.*, Multiplexed Fc array for evaluation of antigen-specific antibody effector profiles. *J. Immunol. Methods* **443**, 33–44 (2017).
89. L. K. Miller-Novak *et al.*, Analysis of complement-mediated lysis of Simian immunodeficiency virus (SIV) and SIV-infected cells reveals sex differences in vaccine-induced immune responses in Rhesus Macaques. *J. Virol.* **92**, e00721-18 (2018).
90. A. J. Hessell *et al.*, Reduced cell-associated DNA and improved viral control in macaques following passive transfer of a single Anti-V2 monoclonal antibody and repeated Simian/human immunodeficiency virus challenges. *J. Virol.* **92**, e02198-17 (2018).

Downloaded from https://www.pnas.org by INSTITUT PASTEUR MEDIATHEQUE SCIENTIFIC on July 19, 2023 from IP address 157.99.174.25.